DOI: 10.1002/chem.200902452

How Post-Translational Modifications Influence Amyloid Formation: A Systematic Study of Phosphorylation and Glycosylation in Model Peptides

Malgorzata Broncel, Jessica A. Falenski, Sara C. Wagner, Christian P. R. Hackenberger, and Beate Koksch*[a]

Abstract: A reciprocal relationship between phosphorylation and O-glycosylation has been reported for many cellular processes and human diseases. The accumulated evidence points to the significant role these post-translational modifications play in aggregation and fibril formation. Simplified peptide model systems provide a means for investigating the molecular changes associated with protein aggregation. In this study, by using an amyloid-forming model peptide, we show that phosphorylation and glycosylation can affect folding and aggregation kinetics differently. Incorporation of phosphoserines, regardless of their quantity and position, turned out to be most efficient in preventing amyloid formation, whereas O-glycosylation has a more subtle effect. The introduction of a single β-galactose does not change the folding behavior of the model peptide, but does alter the aggregation kinetics in a site-specific manner. The presence of multiple galactose residues has an effect similar to that of phosphorylation.

Keywords: aggregation · coiled coils · glycopeptides · protein folding · protein models

Introduction

Phosphorylation and glycosylation are major post-translational modifications of cellular proteins. These reversible, covalent modifications have an impact on diverse properties of a protein, ranging from subcellular localization and binding to interactions with other proteins. Because phosphorylation and O-glycosylation both target hydroxyl-group-containing amino acids, a reciprocal relationship between these modifications has been suggested.[1] Many reports document that phosphate and O-linked β-*N*-acetylglucosamine (*O*-GlcNAc) alternatively occupy the same or adjacent hydroxyl moieties.[2,3] This finding led to the hypothesis that this sugar may be a temporary site-blocker or a competitor of phosphorylation. In fact, a dynamic interplay between O-glycosylation and O-phosphorylation has been reported for numerous cellular processes (transcription and translation) and human diseases (cancer or diabetes).[4] The accumulated evidence highlights the role of post-translational modifications in the protein aggregation that leads to neurodegeneration.[5] In Alzheimer's disease (AD), for example, abnormally phosphorylated tau protein aggregates lead to the formation of neurofibrillary tangles, one of the hallmark brain lesions responsible for neuron death.[6] It has been shown that tau is also modified by O-glycosylation and that this modification regulates the phosphorylation of tau in a site-specific manner.[7] The underlying molecular mechanisms, however, are still largely unknown. Another AD-related protein, the β-amyloid precursor protein, has also been found to be modified in its cytoplasmic domain by both phosphorylation and glycosylation.[8] However, the exact role of these specific modifications remains to be elucidated.

Despite the great number of studies conducted to date, neurodegeneration is still one of the least understood processes, which is mostly due to the complex nature of molecular interactions as well as the challenging physicochemical properties of naturally aggregating systems. In particular, the low solubility of the proteins involved, their tendency to aggregate, and their difficult synthesis often preclude detailed structural characterization. To overcome these obstacles, the application of simplified peptide model systems is of great interest.[9] Because it has been shown that amyloid formation is a general feature of peptides and proteins,[10] including various non-disease-related proteins, many groups

[a] M. Broncel,[+] J. A. Falenski,[+] Dr. S. C. Wagner, Dr. C. P. R. Hackenberger, Prof. Dr. B. Koksch
Institut für Chemie und Biochemie
Freie Universität Berlin
Takustrasse 3, 14195 Berlin (Germany)
Fax: (+49) 30-838-55644
E-mail: koksch@chemie.fu-berlin.de

[+] These authors contributed equally to this work.

Supporting information for this article is available on the WWW under http://dx.doi.org/10.1002/chem.200902452.

have directed their efforts towards developing simplified models for the studying of aggregation in response to diverse stimuli, including pH,[11,12] temperature,[13] metal ions,[14] and hydrophobic defects.[15] However, to our knowledge, only a few reports describe the influence of phosphorylation and glycosylation by using the same model system.[16–18] Liang et al. used a 38-residue α-helical hairpin peptide (α-helix/turn/α-helix), which transforms from its initial monomeric state to an amyloid at elevated temperature, as a model system to explore how post-translational modifications affect the conformational properties and kinetics of amyloid formation.[16] They found that the principal effect of glycosylation and phosphorylation is to slow down the peptide fibrillogenesis, with the greater effect induced by glycosylation. However, the conformational differences induced by a single sugar or phosphate group introduced into the flexible loop region (Thr19) of the helix–turn–helix model peptide did not have a great effect on the overall structure.

In contrast with the above-mentioned strategy, our group has recently shown that structural changes in amyloid-forming model peptides can be initiated without thermal activation.[11,19,20] We have explored the α-helical coiled coil folding motif, which is very common in nature and has been extensively studied in recent years, proving its application as a reliable model system.[9,11,19,20,41] Furthermore, the design principles of coiled coils are very well understood,[21] and folding is based on oligomerization, which is also the foundation of amyloid formation. Coiled coils consist of at least two α-helices wrapped around each other in a slight superhelical twist. The primary structure is characterized by a periodicity of seven residues, the so-called heptad, which is commonly denoted $(a\text{-}b\text{-}c\text{-}d\text{-}e\text{-}f\text{-}g)_n$ (Figure 1). Positions a and d are typically occupied by nonpolar residues that form the first recognition domain by hydrophobic core packing ("knobs-into-holes"). Charged amino acids at positions e and g form the second recognition motif and engage in interhelical electrostatic interactions. Polar residues are often found at the remaining heptad repeat positions b, c, and f, which are solvent exposed.

Herein, we have used a de novo designed coiled-coil peptide that can form amyloids in a time-dependent fashion as a simplified model for deciphering the impact of two ubiquitous post-translational modifications, phosphorylation and O-linked glycosylation, on the amyloid formation process. Specifically, we have examined the effect of site-specific and multiple phosphorylation to mimic the pattern observed in vivo. Furthermore, β-galactose was incorporated into the same sequence positions. Although β-galactose is not directly linked to serine in eukaryotes, it is commonly occurring at the end positions in glycans.[22] Here, we used β-galactose as an easily accessible residue that serves as a model to study the impact of O-linked sugars on folding. Therefore, O-linked β-galactose was used as a general phosphorylation-site blocker.

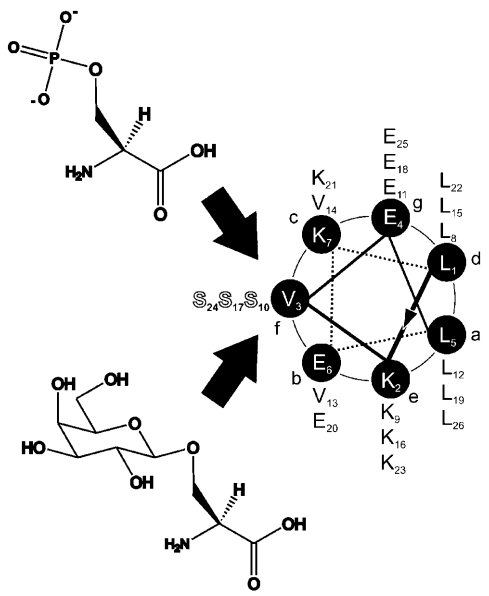

Figure 1. Helical wheel representation of the PP. Black arrows indicate the phosphorylation and glycosylation sites.

The key design features of our model peptide (Figure 1) are as follows: 1) hydrophobic leucine residues at positions a and d in combination with interhelical electrostatic attractions between glutamate and lysine at positions e and g ensure stability of the α-helical coiled-coil structure and 2) amino acids at positions b, c, and f have a minor effect on the stability of the coiled coil; therefore, these positions have been used to incorporate three valine residues that make the system prone to amyloid formation. The resulting peptide contains elements of two competing secondary structures: α helix and β sheet.[20] The effect of post-translational modification of the parent peptide (PP) has been investigated by the introduction of phosphorylation and O-glycosylation into position f of the coiled coil (Ser10, 17, and 24; Table 1). Various complementary spectroscopic and analytical techniques have been used to fully characterize the behavior of our model system.

Results

Circular dichroism spectroscopy: To investigate structural changes associated with post-translational modifications,

Table 1. Sequences of the coiled-coil-based model peptides.

Peptide	Sequence
PP	Abz-LKVELEKLKSELVVLKSELEKLKSEL
p10	Abz-LKVELEKLK**pS**ELVVLKSELEKLKSEL
p17	Abz-LKVELEKLKSELVVLK**pS**ELEKLKSEL
p10/17	Abz-LKVELEKLK**pS**ELVVLK**pS**ELEKLKSEL
g10	Abz-LKVELEKLK**(Gal-)S**ELVVLKSELEKLKSEL
g17	Abz-LKVELEKLKSELVVLK**(Gal-)S**ELEKLKSEL
g10/17	Abz-LKVELEKLK**(Gal-)S**ELVVLK**(Gal-)S**ELEKLKSEL
g10/17/24	Abz-LKVELEKLK**(Gal-)S**ELVVLK**(Gal-)S**ELEKLK**(Gal-)S**EL

time-dependent circular dichroism spectroscopy (CD) measurements were performed at pH 7.4 and peptide concentrations of 100 μM at room temperature. A disaggregation assay using hexafluoroisopropanol (HFIP) was performed with all peptides prior to use to ensure a comparable starting condition. Thus, all aggregates formed during peptide purification were disrupted. As shown in Figure 2a, the PP at the initial time point (0 h) shows two minima at $\lambda = 208$ and 222 nm that are characteristic for α-helical coiled coils. Within 24 h, the peptide undergoes a structural conversion to a β-sheet, identifiable by the presence of a single minimum at $\lambda =$ 216 nm. Concomitantly, a white precipitate was observed, suggesting fibril formation. This structural transition confirms that the PP is a suitable model for studying the effect of phosphorylation and glycosylation on protein conformation.

Dramatic changes in peptide structure are induced by phosphorylation. Regardless of the number and position of the substitution, peptides p10, p17, and p10/17 show complete unfolding. Furthermore, a random-coil conformation is observed for the duration of the experiment (Figure 2b–d). In contrast, incorporation of a single Gal (peptide g10) apparently does not perturb the initial helical structure. The time-dependent behavior of g10 resembles that of PP; however, the structural α-to-β transition is significantly delayed, which might suggest an increase in the stability of the initial α-helical structure. White precipitate was observed after 10 d of incubation. We have also analyzed the influence of a single glycosylation in terms of position in PP sequence. The folding behavior of peptide g17 turns out to be similar to that of g10, with the initial helical structure and time-dependent transition to a β-sheet. However, the kinetics of the conformation switch is faster than for peptide g10. Here, structural conversion is complete within 48 h (see the Supporting Information). Peptides g10/17 and g10/17/24, containing two or three Gal units, respectively, were mostly unfolded. No conformational transition was observed for these multiply glycosylated peptides (Figure 2b–d).

The helical content of all peptides was calculated by using the characteristic CD signal at $\lambda = 222$ nm (Figure 3). PP has a mean residue ellipticity of −27440, which corresponds to a helical content of 77%. The helical content of g10 is slightly higher, which further points to sugar-induced stabilization of the initial fold. This effect, however, is evidently site specific because the helical content of g17 is reduced to 46%. Multiple glycosylation in peptide g10/17 and g10/17/24 clearly destabilizes the helical structure, resulting in only 22 and 12% helicity, respectively. As described above, phosphorylation promotes global unfolding and leads to a dramatic reduction in helical content to 12 and 15% for p10 and p17, respectively. Peptide p10/17 shows the lowest helical content (7%).

ThT binding assay: Because CD spectroscopy does not provide information about amyloid fibril formation, we performed a Thioflavin T (ThT) binding assay to investigate

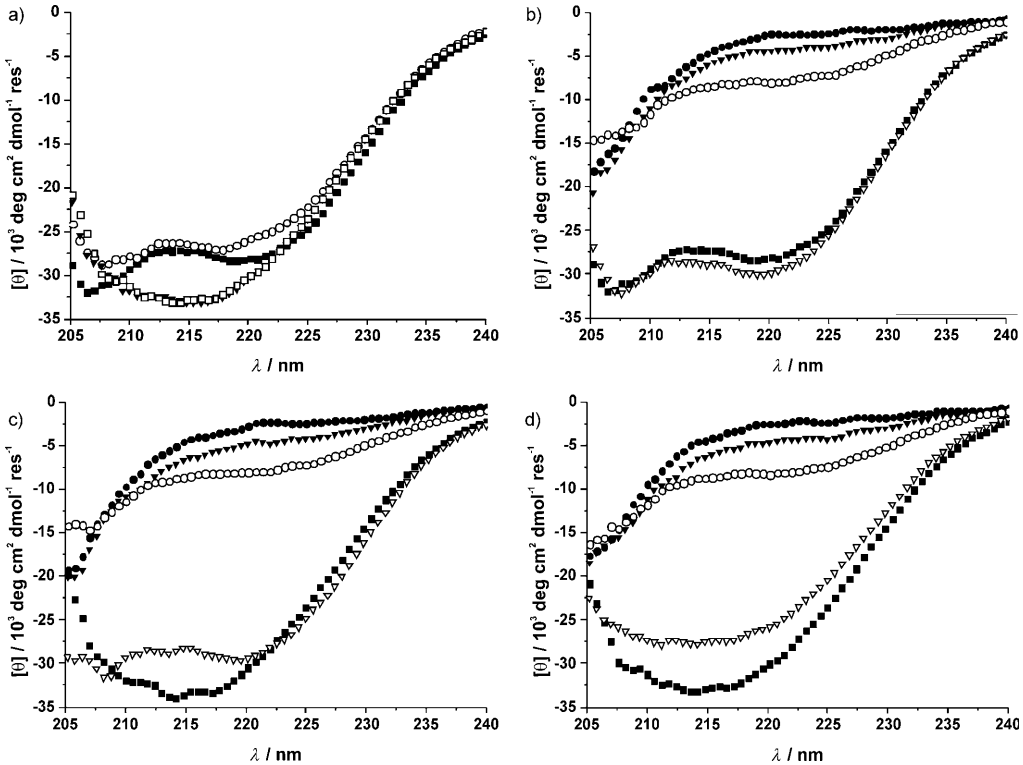

Figure 2. Time-dependent CD spectra of peptides (100 μM) in tris(hydroxymethyl)aminomethane (Tris)/HCl buffer (20 mM; pH 7.4), with NaN_3 (0.025%) at 20°C: Folding behavior of a) the parent peptide (■: 0 h; ○: 6 h; ▼: 24 h; □: 2 weeks) and b–d) peptides PP (■), p10 (▼), p10/17 (●), g10 (▽), and g10/17 (○) immediately after dissolution (b), after 1 week of incubation (c), and after 2 weeks of incubation (d). For CD spectra of peptides p17, g10/17/24, and detailed spectra of g10 and g17 see the Supporting Information.

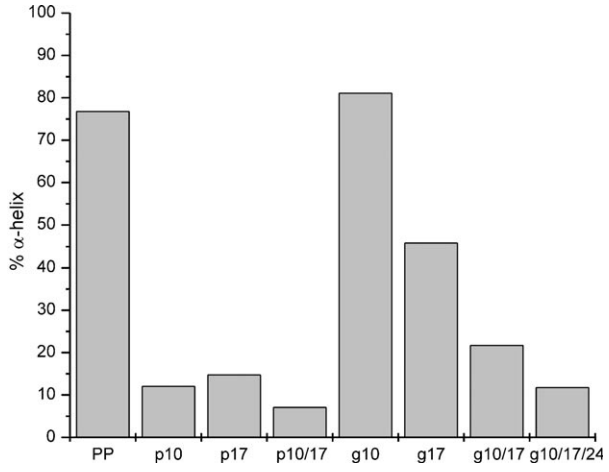

Figure 3. Calculated helical content of peptides used in this study.

whether the observed β-sheet structures are amyloidogenic. ThT exhibits enhanced fluorescence upon binding to amyloid fibrils, and is frequently used for determination of the kinetics of fibril formation.[23] As depicted in Figure 4, inset, ThT in the presence of PP shows a slow increase in fluorescence intensity during the first 6 h of incubation. This initial phase is followed by a rapid increase until 24 h, after which no further increase is observed (Figure 4). After 150 h, a slight decrease in fluorescence intensity and a white precipitate are observed. Similarly to PP, peptide g10 follows a clearly sigmoidal increase in ThT fluorescence. The curve indicates a slow amyloid formation process. The lag phase persisted for about 70 h, and the plateau is reached after two weeks of incubation. The sigmoidal increase in ThT fluorescence is also observed for peptide g17, but here the kinetics of amyloid formation is much faster than for g10 and resembles more that of PP (see the Supporting Information). As expected, phosphorylated peptides p10, p17, and p10/17, as well as glycosylated peptides g10/17 and g10/17/24, do not show any increase in ThT fluorescence over the course of the experiment (Figure 4). These results are in good agreement with the CD spectroscopy data.

Seeding: Partial and full unfolding have been postulated to initiate the conformational transitions associated with amyloid formation.[24–26] However, the ThT experiment did not detect any amyloid formation for the unfolded peptides (p10, p17, p10/17, g10/17, and g10/17/24) in our case. The presence of a lag phase in the observed amyloid formation of PP and g10 indicates a nucleation-dependent polymerization pathway.[27] Nucleus formation is usually a rate-limiting step in amyloid formation. It is followed by a fast elongation phase, which results in mature amyloids. To exclude the possibility of a prolonged lag phase, seeding experiments were conducted. The addition of preformed fibers is known to shorten or even eliminate the lag phase,[28] and the efficiency of this process seems to correlate with the amino acid sequence similarity between the fibril seed and the protein of interest.[29] Preformed aggregates of PP were added to p10, p17, p10/17, and g10/17. Peptide conformation was characterized by CD spectroscopy, and amyloid formation was investigated by the ThT binding assay as described above. Our results show that all peptides maintain their initial random coil structure over two weeks. Additionally, no increase in ThT fluorescence was observed, therefore no amyloid formation occurred (see the Supporting Information).

Transmission electron microscopy: To characterize the morphology of amyloid fibrils formed by PP and g10, two-week-old samples were stained with 1% phosphotungstic acid (PTA) and investigated by transmission electron microscopy (TEM; Figure 5). For the PP, helically twisted ribbons were

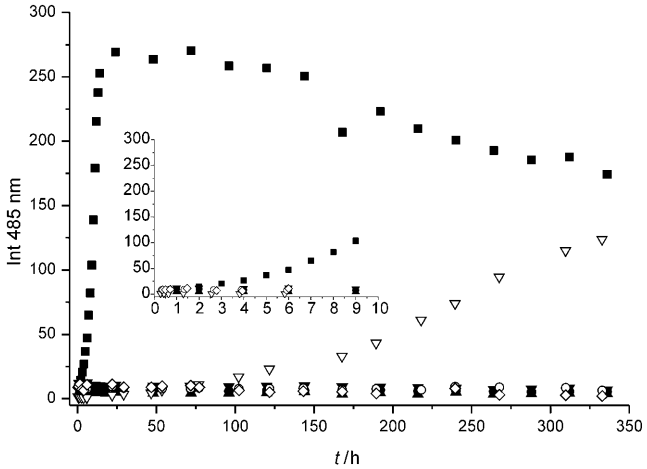

Figure 4. ThT binding assay with peptides (100 μM) PP (■), p10 (▼), p17 (▲), p10/17 (●), g10 (▽), g10/17 (○), and g10/17/24 (◇) in Tris/HCl buffer (20 mM, pH 7.4) with NaN_3 (0.025%) at 20°C; the ThT concentration was 10 μM. One representative data set is shown; experiments were conducted in triplicate. For the ThT assay of peptide g17 see the Supporting Information. Inset: expanded view at short incubation times.

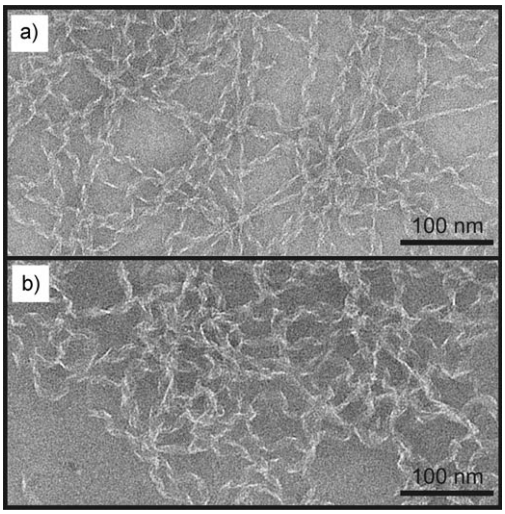

Figure 5. TEM micrographs of matured peptides (100 μM) a) PP and b) g10 prepared in Tris/HCl buffer (20 mM, pH 7.4) with NaN_3 (0.025%). Samples were stained with 1% phosphotungstic acid.

observed. Although the aggregates appear to be similar in their overall morphology, the twisted fibers obviously vary in width, ranging from approximately 3.5 to 9.5 nm. Within these structures, single protofilaments cannot be resolved. Electron microscopic investigation of peptide g10 also showed amyloid-like aggregates, the structural features of which are very similar to those of the PP. Here, we again observe twisted fibers. Nevertheless, in contrast to PP, fibers of smaller width seem to be absent. As expected from the CD and ThT experiments, fibers were also observed for the other monoglycosylated peptide g17 (see the Supporting Information). In this case, however, the peptidic assemblies slightly differ in their overall structural features from both previously discussed peptides. The fibers mainly consist of ribbons that contain laterally assembled protofilaments of 2 to 3 nm in width. Further electron microscopic studies of the other peptides reveal that, in agreement with CD spectroscopic measurements and ThT measurements, no peptide aggregation can be detected (see the Supporting Information).

Discussion

The impact of both post-translational modifications has to be discussed based on two properties: steric bulk and charge. Theoretically, incorporation of a phosphate group into solvent-exposed position f should not destabilize the coiled-coil assembly because neither of the main recognition domains is perturbed. However, this type of substitution, when placed at an interior site in the sequence, could disrupt the intrahelical structure to such an extent that the cooperative interactions that induce helix dimerization cannot take place. This argument has precedent in the literature, and in this case the phosphoserine-mediated destabilization of the monomeric helix was attributed to the high desolvation penalty associated with the bulky side-chain.[30] Szilak et al. have shown this effect in a coiled-coil structure upon phosphorylation at position b,[31] whereas Fujitani et al. reported phosphorylation-dependent destabilization of a helical fragment of H^+/K^+-ATPase.[32] It was also demonstrated that phosphorylation of α-helices can be stabilizing, but only with appropriate neighboring residues.[33,34] Although steric bulk is an important factor associated with the changed folding behavior of the PP, our results imply that it is not the essential factor because the much larger sugar moiety does not lead to the same result. Calculated van der Waals volumes of the native and modified serine side-chains show that phosphorylation increases the side-chain volume by a factor of two, whereas incorporation of a single galactose residue results in a six-fold increase in volume (see the Supporting Information).[35]

The impact of electrostatics on peptide and protein folding and self-assembly has been studied extensively.[11,36,37] Electrostatic interactions involving phosphate, which has a formal charge of −2, are among the strongest interactions involving the standard amino acids and can thus easily perturb the native PP structure. Intramolecular Coulomb repulsions between glutamate (at position b) and phosphate (at position f) destabilize the α-helical coiled coil and as a consequence promote unfolding (Figure 2b–d). Additionally, the excess of uncompensated charge (−2 for single and −4 for double modification) renders the formation and further lamination of β-sheets energetically unfavorable, and thus the peptides remain in solution. The phosphate moiety can be thought of as a "gatekeeper" residue that, when placed in the proximity of the aggregation-prone stretch, prevents its oligomerization.[38] In our study, the ThT binding assay confirms the lack of amyloid formation for all phosphorylated peptides (Figure 4). This result is in agreement with the observations of Lopez de la Paz et al.,[36] who demonstrated the relevance of formal charges to protein oligomerization and fibril formation and suggested that aggregation might preferentially take place for specific charge states of the molecule. Additional support for this view comes from other reports that highlight that the ability of peptides and proteins to form fibrils is highly dependent on environmental factors like pH and ionic strength.[11,37]

The influence of glycosylation can be attributed to the steric demand of the sugar moiety and hydrogen bonding. As mentioned above, the incorporation of even a single galactose increases the serine side-chain volume dramatically. The tight packing interactions mediating protein self-assembly into fibrils can thus be disrupted. Hydrophobic packing interactions similar to those involved in fibril formation are also essential for helix association in coiled-coil structures. Mehta et al. have introduced an O-glycosylated threonine residue into a coiled-coil folding motif to investigate the influence of glycosylation on the stability of α-helical peptides.[39] It was shown that the introduction of a single monosaccharide into a hydrophobic core position disrupts the native coiled-coil structure completely. Furthermore, carbohydrate hydroxyl groups can be involved in hydrogen bonding. One explanation for the observed destabilization of β-sheet structure could be that these hydrogen bonds (addressing backbone amides) compete with the stabilizing intermolecular hydrogen-bonding pattern. Baltzer and coworkers reported such a phenomenon for the molten globule-like helix-loop-helix dimer that was destabilized upon O-glycosylation in close proximity to the hydrophobic core.[40] The decrease in helical content, which led to dimer dissociation, was attributed to the combination of hydrogen bonding and hydrophobic effects. In solvated positions, however, hydrogen bonding is expected to play a minor role.[41] Because the galactose residues are incorporated into the solvent-exposed face of the coiled-coil helices, hydrogen bonding to the peptide backbone will have a negligible effect on this particular conformation. However, in the hydrophobic environment of β-sheets, sugar competition for intermolecular hydrogen bonds will have a distinct destabilizing effect on the overall integrity of this structure.

By using a simplified peptide model system in this study, we have found that phosphorylation and glycosylation have a significant effect on conformation and tendency to form

amyloids. Contrary to previous reports,[16–18] our results clearly show that modification of the model even at single solvent-exposed positions can have a significant impact on peptide structure and the kinetics of amyloid formation. Single and multiple phosphorylation perturb the helical structure and are sufficient to completely abolish amyloid formation. Furthermore, even though single glycosylation does not change the folding behavior of the model peptide, it can effectively alter the aggregation kinetics in a site-specific manner. Multiple modifications with galactose have an effect similar to that of phosphorylation.

The results of our study, albeit rational and transparent, remain difficult to generalize. The effects of phosphorylation on proteins in vivo are known to be highly sequence- and site-specific. For example, studies on phosphorylated tau protein demonstrated that modification at Ser396 and Ser422 promotes aggregation, whereas phosphorylation at Ser262 and Ser214 protects against self-assembly.[42] Moreover, phosphorylation of unstructured peptides derived from the proline-rich region of tau (residues 174–242) induces a conformational transition to a type II polyproline helix.[43] Likewise, the influence of glycosylation seems to be strongly dependent on the nature of the sugar. In this study, easily accessible β-Gal was used as a model for O-linked sugars and as hydroxyl side-chain blocker. However, other sugars have been shown to have diverse effects. Previous studies on O-glycosylated prion protein (PrP) fragments revealed that even the orientation of a single hydroxyl group at the C4 of the sugar can dictate the process of fibril formation.[44] Additionally, it was shown that a N-linked glycan can also indirectly reduce the rate of fibril formation of a PrP-fragment by promoting intermolecular disulfide formation.[45]

Conclusion

Post-translational modifications of proteins play a key role in their structure, function, and stability. They have been implicated in disease-related aggregation processes. Our results demonstrate that amyloid formation can be abrogated by single phosphorylation and multiple glycosylation of serine residues. Despite the mentioned limitations, the experiments described herein certainly shed new light on the complex subject of post-translational modifications and their impact on aggregation. Taking into account the differential influence of various carbohydrates on protein aggregation, further studies addressing *O*-GlcNAc-modified model peptides are currently being conducted in our laboratory.

Experimental Section

Synthesis of N^{α}-(9-fluorenylmethoxycarbonyl)-3-*O*-(2,3,4,6-tetra-*O*-acetyl-β-D-galactopyranosyl)-L-serine: The building block for solid phase peptide synthesis (SPPS) was synthesized by following the procedure of Kihlberg and co-workers.[46] Galactosepentaacetate (2.73 g, 7 mM) and Fmoc-L-Ser-OH (2.89 g, 8.37 mM) were dissolved in MeCN (70 mL), and BF_3·Et_2O (2.64 mL, 21 mM) was added slowly under a N_2 atmosphere and stirred for 1 h at RT. The reaction mixture was then diluted with CH_2Cl_2 and washed with 1 M HCl (3×50 mL) and H_2O (2×50 mL). The organic phase was dried with $MgSO_4$ and concentrated by rotary evaporation. The crude product was purified by preparative reversed-phase HPLC by using a Knauer Smartline system (Knauer, Berlin, Germany) equipped with a Luna C8 column (10μ, 250×21.20 mm; Phenomenex, Torrance, CA, USA) running with a 0.1% trifluoroacetic acid (TFA) in MeCN and 0.1% TFA in H_2O gradient at 20 mL min^{-1}. In each run, the crude product (250 mg) was dissolved in MeCN (1 mL) and injected. The organic and aqueous layers of the combined fractions were evaporated, and the product was dissolved in CH_2Cl_2 to give the title compound as a white powder upon concentration under vacuum (2.18 g, 47%). For NMR spectroscopy and ESI-MS details, see the Supporting Information.

Peptide synthesis, purification, and characterization: Peptides were synthesized by using a SyroXP-I peptide synthesizer (Multi-SynTech, Witten, Germany) according to standard Fmoc/*t*Bu chemistry. Preloaded Fmoc-Leu-Wang resin was used for all peptides. For standard couplings, a four-fold excess of amino acid and coupling reagents [*O*-(benzotriazol-1-yl)-*N*,*N*,*N*′,*N*′-tetramethyluronium tetrafluoroborate/1-hydroxybenzotriazole (TBTU/HOBt)] and an eight-fold excess of *i*Pr_2EtN relative to resin loading was used. All couplings were performed as double couplings (30 min). The coupling mixture also contained 0.23 M $NaClO_4$ to prevent on-resin aggregation. Glycosylated and phosphorylated amino acids were coupled manually. Fmoc-Ser(β-D-Gal(Ac)$_4$)-OH was activated by using diisopropylcarbodiimide/1-hydroxy-7-azabenzotriazole (DIC/HOAt) without the addition of base to prevent racemization and an unintended removal of the sugar protecting groups. The molar excess of Fmoc-Ser(β-D-Gal(Ac)$_4$)-OH and coupling reagents was reduced to 1.5-fold for the first coupling and 0.5-fold for the second coupling, and the reaction time was extended to 3 h. Fmoc-Ser(PO(OBzl)OH)-OH was activated with *O*-(7-azabenzotriazol-1-yl)-*N*,*N*,*N*′,*N*′-tetramethyluronium hexafluorophosphate (HATU)/*i*Pr_2EtN. Molar excess of the amino acid and HATU was reduced to two-fold for the first coupling and one-fold for the second coupling. *i*Pr_2EtN was added in three-fold excess with respect to the amino acid and HATU. The reaction time was extended to 6 h. A mixture of 1,8-diazabicyclo[5.4.0]undec-7-ene (DBU) and piperidine (2% each) in DMF was used for Fmoc deprotection (4×5 min). Peptides were cleaved from the resin by treatment with TFA/*i*Pr_3SiH/H_2O (90/9/1; 2 mL) for 3 h. The resin was washed twice with TFA (1 mL) and CH_2Cl_2 (dry, 1 mL), and excess solvent was removed by evaporation. The peptides were precipitated with cold Et_2O, pelleted by centrifugation, and dried under vacuum. Glycopeptides were deacetylated by treatment with sodium methanolate (20 mM in MeOH, pH 11) overnight. Thereafter the pH was adjusted to 4 by addition of concentrated HOAc, and the solvent was evaporated. Purification of all peptides was carried out by preparative reversed-phase HPLC as described above. Purified peptides were characterized by using analytical HPLC and ESI-MS. The analytical HPLC was carried out with a VWR-Hitachi Elite LaChrome system (VWR, Darmstadt, Germany) equipped with a Luna C8 column (5μ, 250×4.6 mm; Phenomenex, Torrance, CA, USA). Peptide mass to charge ratios were measured by using an Agilent 6210 ESI-TOF (Agilent Technologies, Santa Clara, CA, USA) and are given in the Supporting Information.

Concentration determination: Peptide concentrations were estimated by UV spectroscopy by using a Cary 50 UV/Vis spectrometer (Varian, Palo Alto, CA, USA) by using the absorption maximum at $\lambda = 320$ nm of anthranilic acid (Abz) present at the N terminus. A calibration curve was recorded by using different concentrations of H_2N-Abz-Gly-OH·HCl. Lyophilized peptide was dissolved in HFIP (≈2 mg mL^{-1}) and sonicated for 15 min to dissolve all aggregates. Stock solution (50 μL) was dried under an argon flow and phosphate buffer (1 mL; 100 mM, pH 7.4) was added. This peptide solution was transferred into a disposable cuvette with a 1 cm path length and the UV spectrum was recorded. After calculation of the peptide concentration, the stock solution was aliquoted into glass vials and the HFIP was removed under argon flow. The samples were stored at −20 °C prior to use.

Circular dichroism: CD spectra were recorded by using a Jasco J-810 spectropolarimeter (Jasco, Gross-Umstadt, Germany) at 20 °C by using

quartz cuvettes with 0.1 cm path length. The spectra were averaged over three scans ($\lambda = 190$–240 nm, 0.2 nm intervals, 1 nm bandwidth, 1 s response time) and background corrected. Ellipticity was normalized to concentration (c [mol L^{-1}]), number of residues ($n = 27$, including the N-terminal label Abz), and path length (l [cm]) by using Equation (1), in which θ_{obs} is the measured ellipticity in millidegrees and $[\theta]$ is the mean residue ellipticity in 10^3 deg cm^2 dmol^{-1} residue^{-1}.

$$[\theta] = \theta_{obs}/(10000 \times l \times c \times n) \quad (1)$$

Samples were dissolved immediately before measurement in buffer (200 μL; 20 mM Tris/HCl, pH 7.4, 0.025 % NaN_3) to give 100 μM peptide concentrations. The pH was adjusted to 7.4 by addition of 1 M NaOH. For seeding experiments, 1 vol % (2 μL, 100 μM) of pre-incubated (2 weeks) PP solution (fibrils confirmed by TEM) was added to the samples.

ThT-fluorescence spectroscopy: Fluorescence spectra were recorded by using a luminescence spectrometer LS 50B (Perkin–Elmer, Boston, MA, USA) with a 1 cm quartz cuvette. Spectra were recorded from $\lambda = 470$ to 520 nm at RT after excitation at $\lambda = 450$ nm (ex. slit 5 nm, em. slit 20 nm, scan speed 500 nm min^{-1}, accumulations 10) and background corrected. Samples were dissolved immediately before measurement in buffer (500 μL; 20 mM Tris/HCl, pH 7.4, 10 μM ThT, 0.025 % NaN_3) to give a peptide concentration of 100 μM. The pH was adjusted to 7.4 by addition of 1 M NaOH. For seeding experiments, 1 vol % (5 μL, 100 μM) of preincubated (2 weeks) PP solution (fibrils confirmed by TEM) was added to the samples.

TEM: Peptides from CD spectroscopy measurement were examined after two weeks by TEM. Aliquots (6 μL) of the corresponding solution were placed for 60 s on glow-discharged (60 s plasma treatment at 8 W in a BALTEC MED 020) carbon-coated collodium support films covering 400-mesh copper grids (BAL-TEC, Lichtenstein). After blotting and negative staining with phosphotungstic acid (PTA, 1 %), the grids were left to air-dry. TEM images were recorded with a Philips CM12 transmission electron microscope (FEI, Oregon, USA) at 100 kV accelerating voltage and at primary magnification 58000× on Kodak SO-163 negative film by using a defocus of 0.9 nm. Image J (version 1.38x, Wayne Rasband, USA) was used for the determination of the diameter of peptide fibers.

Calculation of α-helicity: The helical content of all peptides was calculated by using the characteristic CD mean residue ellipticity $[\theta]$ at $\lambda = 222$ nm in deg cm^2 dmol^{-1}. The respective value for 100 % helicity in a 27-residue peptide was calculated by using Equations (2) and (3):

$$[\theta]^n_H = -39500 \times (1 - 2.57/n) \quad (2)$$

$$[\theta]^{27}_H = -35740 \quad (3)$$

in which $[\theta]^n_H$ and -39500 are the mean residue ellipticities of a helix of n and infinite residues at $\lambda = 222$ nm in deg cm^2 dmol^{-1}, 2.57 is a chain-length-dependent factor at $\lambda = 222$ nm, and n is the number of residues.[47]

Acknowledgements

We are grateful to the Deutsche Forschungsgemeinschaft (SFB 765: Multivalency as chemical organization and action principle) for financial support. We would also like to thank Dr. Allison Berger for proofreading the manuscript.

[1] G. W. Hart, *Annu. Rev. Biochem.* **1997**, *66*, 315–335.
[2] K. Kamemura, B. K. Hayes, F. I. Comer, G. W. Hart, *J. Biol. Chem.* **2002**, *277*, 19229–19235.
[3] W. G. Kelly, M. E. Dahmus, G. W. Hart, *J. Biol. Chem.* **1993**, *268*, 10416–10424.
[4] F. I. Comer, G. W. Hart, *J. Biol. Chem.* **2000**, *275*, 29179–29182.
[5] C. X. Gong, F. Liu, I. Grundke-Iqbal, K. Iqbal, *J. Neural Transm.* **2005**, *112*, 813–838.
[6] A. Alonso, T. Zaidi, M. Novak, I. Grundke-Iqbal, K. Iqbal, *Proc. Natl. Acad. Sci. USA* **2001**, *98*, 6923–6928.
[7] F. Liu, K. Iqbal, I. Grundke-Iqbal, G. W. Hart, C. X. Gong, *Proc. Natl. Acad. Sci. USA* **2004**, *101*, 10804–10809.
[8] L. S. Griffith, M. Mathes, B. Schmitz, *J. Neurosci. Res.* **1995**, *41*, 270–278, and references therein.
[9] K. Pagel, B. Koksch, *Curr. Opin. Chem. Biol.* **2008**, *12*, 730–739, and references therein.
[10] M. Stefani, C. M. Dobson, *J. Mol. Med.* **2003**, *81*, 678–699.
[11] K. Pagel, S. C. Wagner, R. Rezaei Araghi, H. von Berlepsch, C. Böttcher, B. Koksch, *Chem. Eur. J.* **2008**, *14*, 11442–11451.
[12] J. P. Schneider, D. J. Pochan, B. Ozbas, K. Rajagopal, L. Pakstis, J. Kretsinger, *J. Am. Chem. Soc.* **2002**, *124*, 15030–15037.
[13] B. Ciani, E. G. Hutchinson, R. B. Sessions, D. N. Woolfson, *J. Biol. Chem.* **2002**, *277*, 10150–10155.
[14] K. Pagel, T. Seri, H. von Berlepsch, J. Griebel, R. Kirmse, C. Böttcher, B. Koksch, *ChemBioChem* **2008**, *9*, 531–536.
[15] Y. Takahashi, A. Ueno, H. Mihara, *Bioorg. Med. Chem.* **1999**, *7*, 177–185.
[16] F. C. Liang, R. P. Y. Chen, C. C. Lin, K. T. Huang, S. I. Chan, *Biochem. Biophys. Res. Commun.* **2006**, *342*, 482–488.
[17] J. T. Du, C. H. Yu, L. X. Zhou, W. H. Wu, P. Lei, Y. Li, Y. F. Zhao, H. Nakanishi, Y. M. Li, *FEBS J.* **2007**, *274*, 5012–5020.
[18] C. H. Yu, T. Si, W. H. Wu, J. Hu, J. T. Du, Y. F. Zhao, Y. M. Li, *Biochem. Biophys. Res. Commun.* **2008**, *375*, 59–62.
[19] K. Pagel, T. Vagt, B. Koksch, *Org. Biomol. Chem.* **2005**, *3*, 3843–3850.
[20] K. Pagel, S. C. Wagner, K. Samedov, H. von Berlepsch, C. Böttcher, B. Koksch, *J. Am. Chem. Soc.* **2006**, *128*, 2196–2197.
[21] D. N. Woolfson, *Adv. Protein Chem.* **2005**, *70*, 79–112.
[22] R. G. Spiro, *Glycobiology* **2002**, *12*, 43R-56R.
[23] R. Khurana, C. Coleman, C. Ionescu-Zanetti, S. A. Carter, V. Krishna, R. K. Grover, R. Roy, S. Singh, *J. Struct. Biol.* **2005**, *151*, 229–238.
[24] R. Wetzel, *Acc. Chem. Res.* **2006**, *39*, 671–679.
[25] F. Chiti, P. Webster, N. Taddei, A. Clark, M. Stefani, G. Ramponi, C. M. Dobson, *Proc. Natl. Acad. Sci. USA* **1999**, *96*, 3590–3594.
[26] M. Fandrich, V. Forge, K. Buder, M. Kittler, C. M. Dobson, S. Diekmann, *Proc. Natl. Acad. Sci. USA* **2003**, *100*, 15463–15468.
[27] I. W. Hamley, *Angew. Chem.* **2007**, *119*, 8274–8295; *Angew. Chem. Int. Ed.* **2007**, *46*, 8128–8147.
[28] J. T. Jarrett, P. T. Lansbury, *Cell* **1993**, *73*, 1055–1058.
[29] B. O'Nuallain, A. D. Williams, P. Westermark, R. Wetzel, *J. Biol. Chem.* **2004**, *279*, 17490–17499.
[30] C. D. Andrew, J. Warwicker, G. R. Jones, A. J. Doig, *Biochemistry* **2002**, *41*, 1897–1905.
[31] L. Szilák, J. Moitra, D. Krylov, C. Vinson, *Nat. Struct. Biol.* **1997**, *4*, 112–114.
[32] N. Fujitani, M. Kanagawa, T. Aizawa, T. Ohkubo, S. Kaya, M. Demura, K. Kawano, S. Nishimura, K. Taniguchi, K. Nitta, *Biochem. Biophys. Res. Commun.* **2003**, *300*, 223–229.
[33] N. Errington, A. J. Doig, *Biochemistry* **2005**, *44*, 7553–7558.
[34] L. Szilak, J. Moitra, C. Vinson, *Protein Sci.* **1997**, *6*, 1273–1283.
[35] For a previous investigation, which supports the significant difference in size between a monosaccharide and the phosphate group, see: B. Imperiali, S. E. O'Connor, *Curr. Opin. Chem. Biol.* **1999**, *3*, 643–649.
[36] M. Lopez de la Paz, K. Goldie, J. Zurdo, E. Lacroix, C. M. Dobson, A. Hoenger, L. Serrano, *Proc. Natl. Acad. Sci. USA* **2002**, *99*, 16052–16057.
[37] J. Zurdo, J. I. Guijarro, J. L. Jimenez, H. R. Saibil, C. M. Dobson, *J. Mol. Biol.* **2001**, *311*, 325–340.
[38] M. Lopez de la Paz, L. Serrano, *Proc. Natl. Acad. Sci. USA* **2004**, *101*, 87–92.
[39] S. Mehta, M. Meldal, V. Ferro, J. Ø. Duus, K. Bock, *J. Chem. Soc. Perkin Trans. 1* **1997**, 1365–1374.
[40] S. Vijayalekshmi, S. K. George, L. K. Andersson, J. Kihlberg, L. Baltzer, *Org. Biomol. Chem.* **2003**, *1*, 2455–2460.

[41] J. A. Scheike, C. Baldauf, J. Spengler, F. Albericio, M. T. Pisabarro, B. Koksch, *Angew. Chem.* **2007**, *119*, 7912–7916; *Angew. Chem. Int. Ed.* **2007**, *46*, 7766–7769.
[42] C. X. Gong, F. Liu, I. Grundke-Iqbal, K. Iqbal, *J. Biomed. Biotechnol.* **2006**, *2006*, 1–11, and references therein.
[43] A. A. Bielska, N. J. Zondlo, *Biochemistry* **2006**, *45*, 5527–5537.
[44] P. Y. Chen, C. C. Lin, Y. T. Chang, S. C. Lin, S. I. Chan, *Proc. Natl. Acad. Sci. USA* **2002**, *99*, 12633–12638.
[45] C. J. Bosques, B. Imperiali, *Proc. Natl. Acad. Sci. USA* **2003**, *100*, 7593–7598.
[46] L. A. Salvador, M. Elofsson, J. Kihlberg, *Tetrahedron* **1995**, *51*, 5643–5656.
[47] Y. H. Chen, J. T. Yang, K. H. Chau, *Biochemistry* **1974**, *13*, 3350–3359.

Received: September 4, 2009
Revised: March 24, 2010
Published online: May 20, 2010

